Structural and electronic properties of the fullerene isomers of Si_{38}: A systematic theoretical study

Zacharias G. Fthenakis*

Institute of Electronic Structure and Laser, P.O. Box 1527, Heraklion-Crete 71110, Greece and Department of Physics, University of Crete, Heraklion-Crete 71110, Greece

Remco W. A. Havenith

Theoretical Chemistry Group, Utrecht University, Padualaan 8, 3584 CH Utrecht, The Netherlands

Madhu Menon

Department of Physics and Astronomy, University of Kentucky, Lexington, Kentucky 40506-0055, USA and Center for Computational Sciences, University of Kentucky, Lexington, Kentucky 40506-0055, USA

Patrick W. Fowler

Department of Chemistry, University of Sheffield, Sheffield S3 7HF, United Kingdom

A systematic study of the structural and electronic properties of the 17 Si_{38} fullerene cage isomers, which are constructed by making all possible permutations among their pentagons and hexagons, is presented. For the full optimization of these structures, a tight-binding molecular-dynamics method is firstly applied, and the resulting structures were further optimized with two more accurate but more time-consuming methods, namely, the generalized tight-binding molecular dynamics and a density-functional theory calculation at the B3LYP level. In addition, the Si_{20} fullerene cage, optimized with the same methods, is also presented for comparison. The results of all these methods are in good agreement with each other, and they all predict the same isomer as the energetically most stable structure among these 17 isomers. In all the fullerene isomers, half of the atoms are nearly coplanar with their three neighbors, and half lie on sharp corners of the polyhedral cage, coinciding with a distinction between half of the atoms adopting an sp^2-like hybridization and the other half using essentially pure p orbitals in their bonding to nearest neighbors.

PACS number(s): 81.05.Tp, 61.46.Df, 73.22.−f, 33.15.Dj

I. INTRODUCTION

The interest in fullerene structures can be traced to the discovery of buckminsterfullerene in 1985 by Kroto *et al.*[1] By definition, a fullerene cage is a polyhedron with faces consisting only of hexagons and pentagons.[2] As a consequence of Euler's theorem, it can be shown that a fullerene containing N vertices can be constructed from exactly 12 pentagons and $N/2-10$ hexagons. Fullerenes can be constructed with any even number of atoms greater than or equal to 20, with the sole exception of $N=22$.[2]

By gluing together the pentagons and hexagons in all possible different ways, isomers can be constructed, the number of which increases rapidly with the number of atoms (see Ref. 2, p. 32). Amongst the carbon fullerenes, the most well known and most abundant is buckminsterfullerene, C_{60}, in the isomer possessing I_h (icosahedral) symmetry. This is the only isomer of C_{60}, out of 1812, that obeys the "isolated pentagon rule" (IPR),[2,3] and 60 is the smallest atom number at which isolation of pentagons is possible. Isolation is next possible at 70, and for all even atom counts thereafter. The IPR states that the most stable carbon fullerenes are those with all their pentagons separated by hexagons. More generally, the stability of carbon fullerenes correlates well with the number of pentagon-pentagon fusions N_p, the total energy increasing approximately linearly with the number of adjacencies (see Ref. 3 and references therein), and for the lower

fullerenes ($N \leq 68$), the most stable isomer identified in systematic calculations is generally one that contains the minimum possible number of pentagon adjacencies.

Owing to their many unusual properties, carbon fullerenes and their derivatives (nanowires, nanotubes, etc.) are seen as very promising materials for nanotechnology applications.

Silicon is an element in the same group as carbon, but with quite different behavior in forming chemical bonds. For example, the geometrical structures of silicon and carbon clusters are radically different. In the bulk phase, Si prefers to form sp^3 bonds, while C is versatile and exhibits sp^2 and sp^3 bondings and sometimes even sp bonding.

There have been a number of calculations on Si fullerenes (see Refs. 4 and 5 and references therein), from which it emerges that at least some of the cages occupy local minima on the potential-energy surface.

Si fullerenes are interesting structures not only for the better understanding of the properties of the Si trivalent bonding systems but also as possible candidates for the construction of new materials with exotic properties. In addition to Si fullerenes, the Si trivalent bonding behavior has also been seen in some novel nanostructures such as Si nanowires,[6–8] Si nanotubes (see Ref. 9 and references therein), Si surfaces,[10] Si endohedral clusters,[7,11] Si-C heterofullerenes,[12] clathrates,[13,14] etc., all of which are expected to have potential for applications in nanotechnology.

Work related to Si fullerenes to date has been focused on (a) silicon fullerenes which include a core of some Si

atoms,[15–19] with special attention devoted to Si_{45} (see Ref. [15] and references therein and Refs. [16] and [19]); (b) Si_{20} and Si_{60} fullerenes encapsulating a core of a metallic cluster [such as $Al_{12}X@Si_{60}$, $X=Si$, Ge, Sn, Pb, or $Ba@Si_{20}@Si_{60}$ (Ref. [17])] or a metal atom [such as $M@Si_{20}$, $M=Ba$, Sr, Ca, Zr, Pb,[11,20,21] or $X@Si_{60}$, $X=Zn$, Zn^{+2}, Pd, Be, Be^{+2} (Refs. [22–24])]; (c) Si fullerenes hydrogenated to terminate the dangling Si bonds [such as $Si_{20}H_{20}$ (Refs. [20] and [25])]; (d) Si fullerene-based extended systems such as Si clathrates (see, for example, Refs. [13] and [14]), nanowires,[6–8] and nanotubes;[9] and (e) empty Si fullerenes with special attention devoted to icosahedral Si_{60} (Refs. [4], [5], [17], [22–24], and [26–31], also see references therein), although there is still debate about the Si_{60} fullerene structure. Some work has dealt with other types of Si fullerenes, such as Si_{20} (Refs. [21] and [32], also see references therein), Si_{24},[6] Si_{26} and Si_{28},[18,32] Si_{30} and Si_{32},[32] Si_{36},[33] Si_{50},[26,27] and Si_{70}.[27] A recent work by Han *et al.*[34] has presented a systematic theoretical study of some Si_n ($n=26–36,60$) cages, though not all true fullerenes in that many include four-valent atoms.

Calculations on Si fullerenes often begin with highly symmetrical starting structures, which are usually reduced in symmetry upon relaxation. Most isomers will, in fact, have low symmetry: structures such as I_h Si_{60} or Si_{20} are exceptions. The general conclusions arising from these studies are the following: (a) all the Si fullerenes are thermodynamically unstable, representing local rather than global energy minima, and (b) their structures are distorted "puckered" balls.[27] What is lacking so far is a systematic study of all the possible Si fullerenes with a given nuclearity. The present work reports a detailed consideration of the 38-atom Si fullerenes, allowing all mathematically possible arrangements of their 12 pentagons and nine hexagons. There are 17 such isomers.[2] For comparison, a study of Si_{20}, made using the same methods, is also presented.

II. THE OPTIMIZATION METHOD

Bearing in mind the fact that our interest is in the fullerene structures and that we intend to use molecular-dynamics method for this purpose, it is not necessary to make an extensive search over the entire configuration space of the Si_{38} system, but only on the configuration space of the particular fullerene of interest. In other words, our search might be restricted to a small part of the Si_{38} configuration space where the fullerene network of each particular isomer is preserved during the molecular-dynamics procedure. For this restrictive search, an alternative molecular-dynamics method has been developed,[35] for which more details can be found in Ref. [36]. An initial trivalent connection list is conserved by freezing atoms whenever their separation from nominal neighbors threatens to exceed a specified cutoff distance.

To expedite the search for the optimum structure, a simple orthogonal tight-binding Hamiltonian with a fitted repulsive
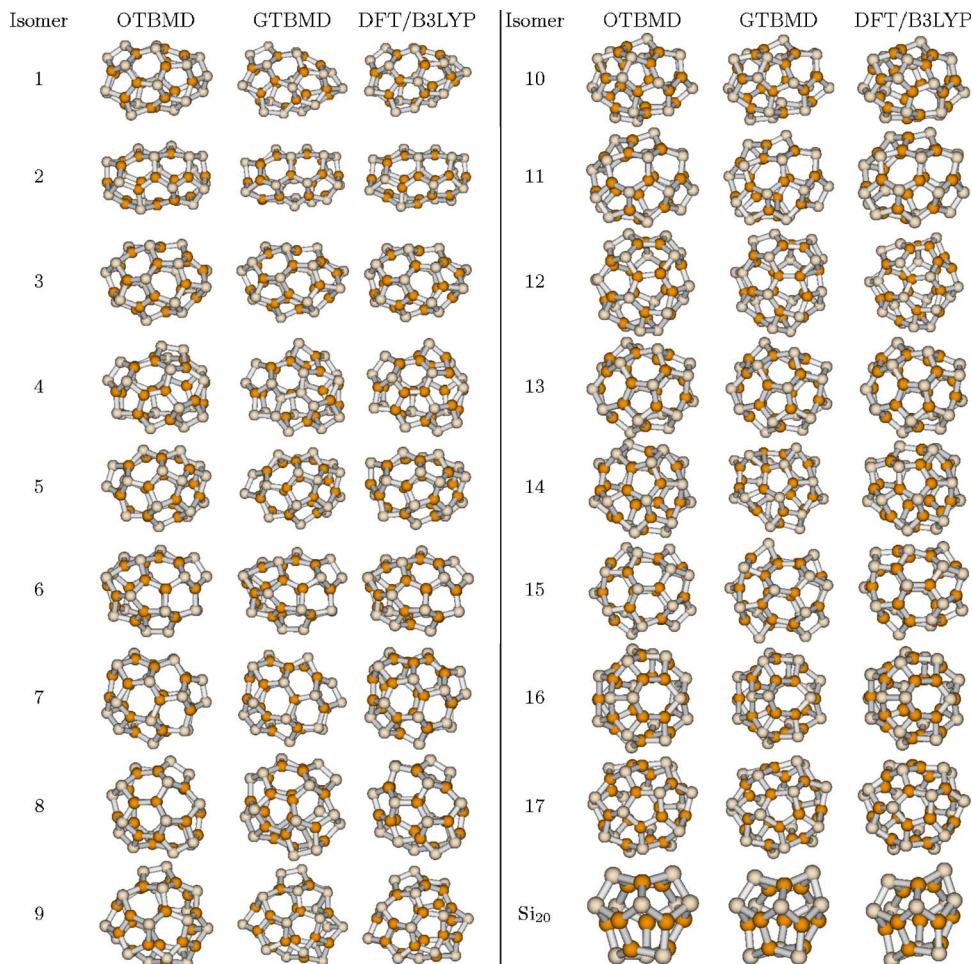

Isomer	OTBMD	GTBMD	DFT/B3LYP	Isomer	OTBMD	GTBMD	DFT/B3LYP
1				10			
2				11			
3				12			
4				13			
5				14			
6				15			
7				16			
8				17			
9				Si_{20}			

FIG. 1. (Color online) The optimum structures of the 17 isomers of Si_{38} and the optimum structure of Si_{20} obtained with the three methods.
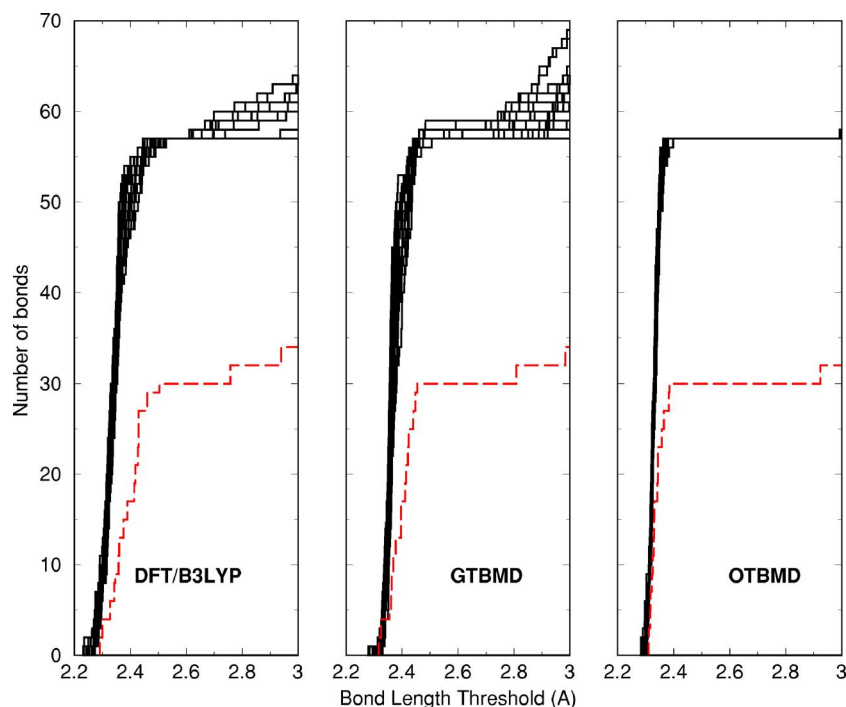
FIG. 2. (Color online) Distribution of bond lengths for the 17 optimized Si_{38} fullerene isomers (solid lines) and for the Si_{20} fullerene (dashed) computed with the three methods (see text for details).

pair potential (see, for example, Ref. 37 and references therein) was used to describe the potential-energy surface of the 17 isomers. The optimum structures found within this method were further optimized with the generalized tight-binding molecular-dynamics (GTBMD) scheme[38] and a density-functional theory (DFT) calculation at the B3LYP level, using a DZP basis set, as implemented in the GAMESS-UK program package.[39]

III. RESULTS AND DISCUSSION

A. Geometrical structure

In Fig. 1, the optimum structures of the 17 Si_{38} fullerene isomers and the Si_{20} fullerene, obtained with the three methods mentioned above, are presented. The numbering for the 17 Si_{38} isomers is identical to the one used in the face-spiral system for carbon fullerenes (see Ref. 2, p. 185). As can be seen, the structures obtained for a given isomer with the three methods differ only slightly from each other. This implies that all the methods can give useful information on structural patterns, although the DFT/B3LYP method may be expected on general grounds to be more accurate than the semiempirical tight-binding methods. As will be discussed below, in comparison with an imagined spherical structure, half of the atoms of every optimized structure have moved radially outward, while the other half have moved inward. This is shown in Fig. 1: atoms that have moved inward are dark colored, and those that have moved outward are light colored. The coordinates of all the structures presented in Fig. 1, can be found in the supplementary information files. (See Ref. 40).

B. Symmetry

Although the 17 isomers, considered as graphs embedded on the sphere, have various maximum point-group symme-

tries, $D_{3h}(1)$, $C_{3v}(1)$, $D_3(1)$, $C_{2v}(1)$, $C_2(5)$, and $C_1(7)$,[2] on optimization, all distort to C_1 symmetry. The Si_{20} fullerene structure, with topologically maximum I_h symmetry, is reduced to C_2 in the orthogonal tight-binding molecular-dynamics (OTBMD) optimization, and on further optimization using the GTBMD and DFT methods, its symmetry is lowered to C_1. These results are in contrast to the findings of Li and Cao[32] who, using a full-potential linear-muffin-tin-orbital molecular dynamics, have reported that the relaxed Si_{20} belongs to the I_h point group. In view of the electron count, which implies a Jahn-Teller distortion for the neutral cluster in I_h symmetry, this reported retention of symmetry is difficult to rationalize.

C. Bond lengths

Figure 2 presents the distributions of bond lengths in the optimized fullerene structures: the number of bonds with length less than a given cutoff is plotted against bond length for the 17 isomers of Si_{38} and the unique Si_{20} for all three methods. From the figure, it is clear that, in terms of bond length, the 17 Si_{38} fullerene isomers do not exhibit any strong variations. The figure identifies 57 (i.e., $3/2 \times 38$) and

TABLE I. Range of the bond lengths of the Si_{38} and Si_{20} fullerenes (in Å).

Method	Si_{38}		Si_{20}	
	From	To	From	To
OTBMD	2.28	2.40	2.31	2.39
GTBMD	2.27	2.51	2.31	2.45
DFT/B3LYP	2.23	2.53	2.29	2.50

TABLE II. Cohesive energies (in meV) of the Si_{38} fullerene isomers, given relative to that of the most stable isomer (9).

Isomer No.	Initial point group	OTBMD	GTBMD	DFT/B3LYP
1	C_2	34.5218	30.1795	22.5986
2	D_{3h}	38.7466	22.9934	41.8480
3	C_1	19.2899	39.7223	28.9318
4	C_1	33.1120	21.1251	23.6871
5	C_1	7.4140	34.6560	29.5995
6	C_2	15.9544	41.0044	27.8750
7	C_1	37.0243	51.4068	44.0675
8	C_1	24.7143	17.9728	14.3652
9	D_3	0	0	0
10	C_2	26.8155	52.9022	38.9243
11	C_1	6.0325	34.3963	28.0246
12	C_{2v}	58.8272	55.5103	42.7501
13	C_2	4.0532	39.3364	23.3851
14	C_1	25.4870	29.3113	22.0791
15	C_{2v}	25.0986	25.6212	34.6025
16	C_{3v}	4.6854	36.9426	27.3989
17	C_2	2.9096	43.9919	20.9670

30 (i.e., $3/2 \times 20$) nearest-neighbor bonds for Si_{38} and Si_{20}, respectively, although in a few Si_{38} isomers, the shortest distances between some (very few) second-nearest neighbors and the longest distances between nearest neighbors are close. The trivalent fullerene network is still preserved, even though the geometry is distorted. The range of bond lengths is presented in Table I. In the DFT/B3LYP calculation, the bonds of the Si_{38} fullerene isomers fall in a range of 0.30 Å, between 2.23 and 2.53 Å, and the bonds of the Si_{20} fullerene themselves span 0.21 Å. The corresponding ranges obtained with the GTBMD and the OTBMD methods are even smaller. GTBMD bond lengths are on average 1.5%–2.5%

larger than those obtained in the DFT/B3LYP calculations.

D. Cohesive energy and optimum isomer

Optimization of the 17 Si_{38} fullerene isomers with the three methods and calculation of the cohesive energy (i.e. binding energy per atom) lead to the prediction of number 38:9 (Ref. 41) (initially of D_3 point-group symmetry) as the most stable of the 17. The relative cohesive energies, as obtained by the three methods, are presented in Table II. These differences are also plotted in Fig. 3, which shows the energy profiles for the GTBMD and DFT/B3LYP methods, illustrating the clear preference for isomer 38:9.

As seen from the plot, the results of the GTBMD and DFT/B3LYP methods are in good agreement with each other. The calculated cohesive energies are concentrated in a range of less than 60 meV, but the difference in cohesive energy between optimum Si_{38} isomer is typically at least 20 meV. It seems that details of the arrangement of pentagonal and hexagonal faces do not, in general, greatly affect their cohesive energy and/or stability. However, isomer 38:9 is clearly preferred over the others. Is there a qualitative explanation for this?

E. On the stability of Si fullerenes

Marsen and Sattler,[6] accounting for their experimental observations of Si nanowires, proposed a model for Si fullerenes. In contrast to carbon fullerenes, it is proposed that the most stable Si fullerenes will be those that maximize the number of pentagon adjacencies. A corollary[6] is that Si_{20}, where N_p takes the maximum possible value of 30, should be the most stable of all Si fullerenes. The present results do not support this inference: the best isomer of Si_{38} is intermediate in cohesive energy between Si_{20} and bulk silicon (Table III). Other workers too have found more that loss of pentagon adjacencies does not always lead to improvement in cohesive energy.
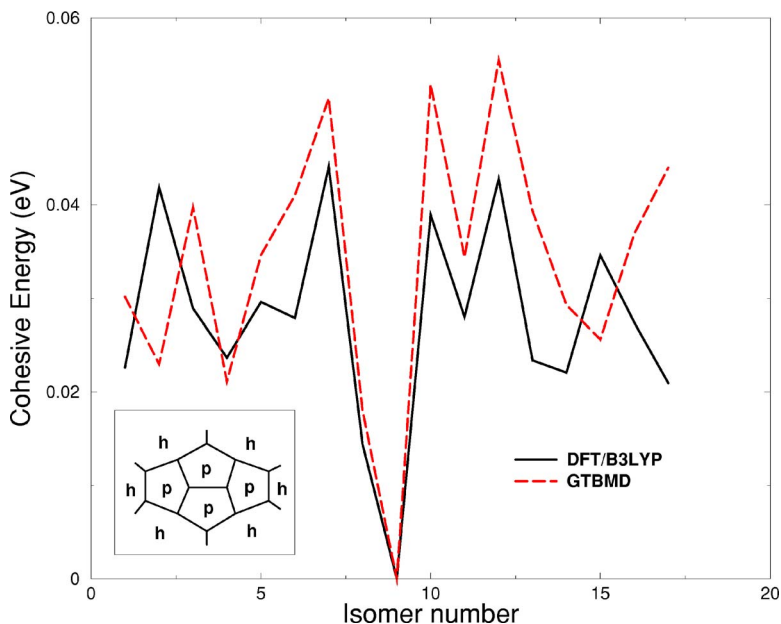

FIG. 3. (Color online) Cohesive energies of the 17 Si_{38} isomers found with (a) DFT/B3LYP (solid line) (b) GTBMD (dashed line). The fused-pentagon-quadruple motif is shown in the inset (p, pentagon; h, hexagon).

TABLE III. Cohesive energies (in eV) of three forms of silicon, calculated using the three methods.

Compound	OTBMD	GTBMD	DFT/B3LYP
Si_{38} (isomer 9)	3.1839	4.1160	3.3226
Si_{20}	3.0668	4.0775	3.2417
Bulk Si	4.64[a]	4.27	

[a]Fitted.

A comparison between the cohesive energies in the work of Cao and co-workers,[4,26,32] using a full-potential linear-muffin-tin-orbital molecular dynamics, for Si_n, n $=20,24,26,28,30,32,50,60$, shows that the cohesive energies do not fall monotonically as the number of atoms increases. In addition,[26] the I_h Si_{60} fullerene (with isolated pentagons) and the Si_{50} fullerene (with five pentagon pairs) are almost isoenergetic, with Si_{60} being more stable than Si_{50} by only 0.01 eV/atom. Also, from our findings in the present work, isomers 2, 3, and 6, which contain more fused pentagons than other Si_{38} isomers, were found to be less stable than other isomers with fewer fused pentagons. Clearly, Si fullerenes tolerate pentagon adjacencies more easily than carbon fullerenes, but it seems that the model of Marsen and Sattler is not predictive in any useful way.

The following question remains: what distinguishes isomer 38:9 from the others? This isomer has a very specific arrangement of its 12 pentagons in the form of three separated fused quadruples (as illustrated in the inset panel of Fig. 3). A Si_{38} isomer, with its nine hexagons, is the smallest in which three such motifs can be separated. Isomer 38:8, which is the second most stable of the 17 isomers, has one such motif. It is tempting to associate the presence of the fused quadruple with stabilization. Investigation of more examples would be needed before any firm conclusion could be drawn.

F. Pentagon and hexagon angle distribution

In the ideal case, a fullerene (seen as a geometrical structure) contains regular pentagons and hexagons, with angles equal to 108° and 120°, respectively. However, such a structure can be constructed only in the cases of highest symmetry: the dodecahedral 20-atom and the truncated icosahedral 60-atom fullerene. For the other cases, edge lengths have some distribution. The distributions of pentagon and hexagon bond angles (i.e., the number of bond angles with values between θ and $\theta+\delta\theta$, with $\delta\theta=1°$) for the 17 Si_{38} fullerene isomers are found to be bimodal, peaking near the values of 90° and 115° (for pentagons) and 100° and 125° (for hexagons), as shown in Fig. 4.

If the pentagon distribution is shifted by +12° [i.e., by the difference of the ideal hexagon angle (120°) from the ideal pentagon angle (108°)] and scaled for the difference between the numbers of $5\times12=60$ pentagon angles and the 6 $\times(N/2-10)=54$ hexagon angles, then the two distributions almost coincide [Fig. 4(c)]. It is worth noting that the number of pentagon angles is always 60 (i.e., 5×12) for any fullerene, but the number of hexagon angles depends on the number of the fullerene nuclearity, i.e., $6\times(N/2-10)=3N-60$. In our case ($N=38$), the number of hexagon angles is 54. Thus, the reduction of the two distributions to the same number of angles may be achieved by multiplying the hexagon angle distribution by 60/54.

Similar pentagon and hexagon angle distributions with those obtained from all the 17 isomers, are obtained from the energetically optimum isomer 38:9 only (see Figs. 1 and 2 of Ref. 40). Nothing particular is found in those figures that would distinguish 38:9 isomer from the others.

G. Local planarity

A measure of flatness of a fullerene structure, locally around a particular atom, is given by the sum $\phi=\theta_1+\theta_2$
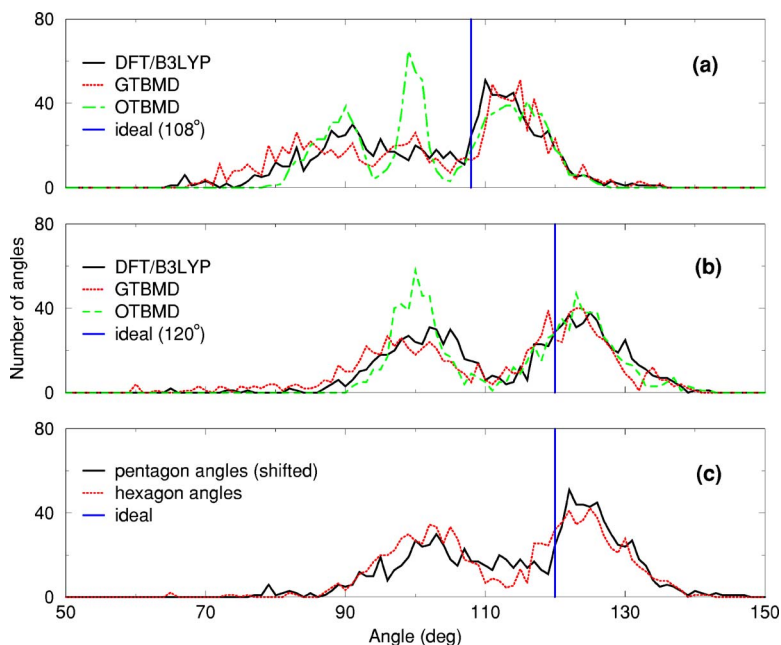

FIG. 4. (Color online) Distribution of the (a) pentagon and (b) hexagon angles for the (I) DFT/B3LYP (solid line), (II) GTBMD (dotted line), and (III) OTBMD (dot-dashed line) calculations. (c) The pentagon (solid line) and the hexagon (dotted line) angle distributions for the DFT calculation, shifting the former by +12° and multiplying the latter by 60/54. These distributions have been calculated for all the 17 Si_{38} fullerene isomers.
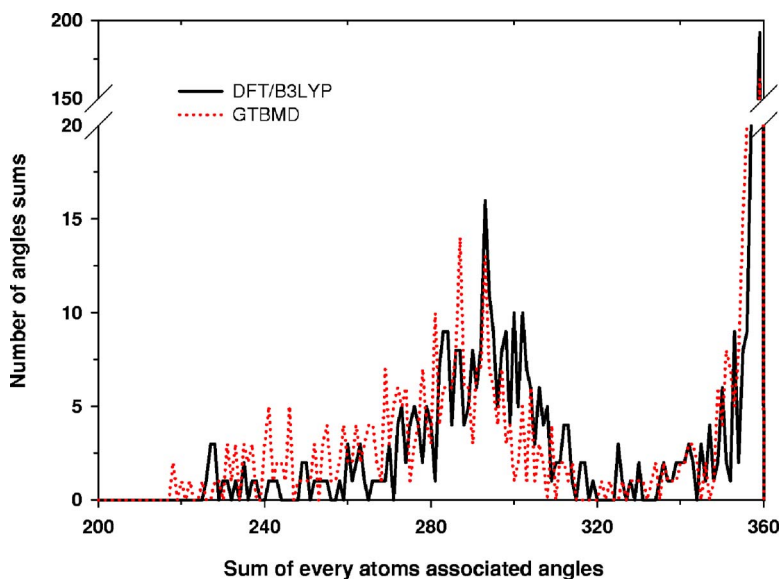
FIG. 5. (Color online) Distribution of the angle sums associated with every atom, for all the atoms of the 17 Si_{38} fullerene isomers, obtained with (a) DFT/B3LYP (solid line) and (b) GT-BMD (dotted line).

$+\theta_3$ of the three bond angles θ_i associated with that atom. If the structure is locally perfectly flat, then this sum will be 360°. For all other cases, this sum will take lower values. For the ideal case for which the fullerene is constructed from regular pentagons and hexagons, this sum (for any particular atom) takes one of four values, 360°, 348°, 336°, or 324°, depending on the number of pentagons to which that atom belongs.

By plotting the distribution of angle sums for all atoms of all isomers, it is found that the distribution consists of two parts (see Fig. 5). For the OTBMD method, these are separated by approximately 32°, from 318° to 350°, with for every Si_{38} isomer, half of the sums above and the half below the gap. The gap is less pronounced in the GTBMD and the DFT calculations, but the values of 341° and 348°, respectively, separate the upper and lower halves of the sums. The higher sums are concentrated near 360° and the lower sums are dispersed around 290° with a wide dispersion (70°–120° depending on the method). The same picture appears for the corresponding distribution of the 38:9 isomer. This is clearly shown in Fig. 3 of the supplementary information (see Ref. 40).

This clearly bimodal distribution in local flatness indicates that half of the atoms (those for which the sums tend to 360°) move radially inward and become coplanar to their nearest neighbors, while the other half (those for which the sums are dispersed around 290°) move radially outward, creating sharp corners. These atomic movements lead to the puckered ball structures reported earlier for the Si fullerenes.[27]

Interestingly, investigations of Si surface reconstruction yield almost the same results. For example, from the investigation on the 1×1 and the 1×2 Si(110) surface reconstruction by Menon *et al.*,[10] it is evident that half of the surface trivalent atoms move inward and become almost coplanar to their three nearest neighbors (one of which belongs to the second layer), while the other half move outward creating sharp corners. Using their calculated angle by which the zigzag surface chains are rotated and the displacements Δy and Δz by which they are translated (see Ref. 10), we

have calculated the sums of the three bond angles associated with each atom. This sum is about 356° for the atoms which move inward, while for the atoms which move outward, it is about 305°. These values, compared to the values found in the present work, are consistent with the Si fullerene results, allowing for bias toward tetrahedral angles for the bulk caused by the presence of a neighbor in the second layer.

It is also worth noting that materials such as $BaSi_2$ are constructed with three-coordinated Si atoms in a puckered planar structure, in which the sp^3 hybridization has been frustrated because of the Ba intercalation between planes.[42] $BaSi_2$ is used in the high-pressure synthesis of silicon clathrates, i.e., networks of small Si fullerenes. Other Si fullerene-like networks with stronger p character have also been described.[42]

H. Hybridization

For the locally planar atoms, the hybridization is clearly close to sp^2. For the other atoms, geometry and hybridization are not tetrahedral sp^3, as might be expected. The average of the three bond angles associated with these atoms is approximately 96.7°, i.e., close to the value of 90°, which indicates essentially pure p bonding of these atoms.

To quantify the hybridization of the Si fullerene orbitals, we note that for every Si atom in the trivalent fullerene, the directions of three hybridized orbitals are those of the bonds. Every hybridized orbital $|h_i\rangle$ has the form $|h_i\rangle = \sqrt{1-n_i}|s\rangle + \sqrt{n_i}|p_i\rangle$, $n_i \in [0,1]$, where $|p_i\rangle = m_x^{(i)}|p_x\rangle + m_y^{(i)}|p_y\rangle + m_z^{(i)}|p_z\rangle$ is the p orbital in the direction $\hat{m}_i = m_x^{(i)}\hat{i} + m_y^{(i)}\hat{j} + m_z^{(i)}\hat{k}$, $[(m_x^{(i)})^2 + (m_y^{(i)})^2 + (m_z^{(i)})^2 = 1]$. By taking hybrids along the three bond directions and applying orthogonality, the fourth orbital can be constructed. These are the same considerations used in the fullerene context in Haddon's POAV2 model.[43]

In a qualitative picture of the bonding, the first three hybrids form strong σ bonds with the hybrids of the neighboring atoms. The fourth hybrid is related to a dangling bond and forms at best a weak π-type bond with the corresponding hybrids of the three neighbors.
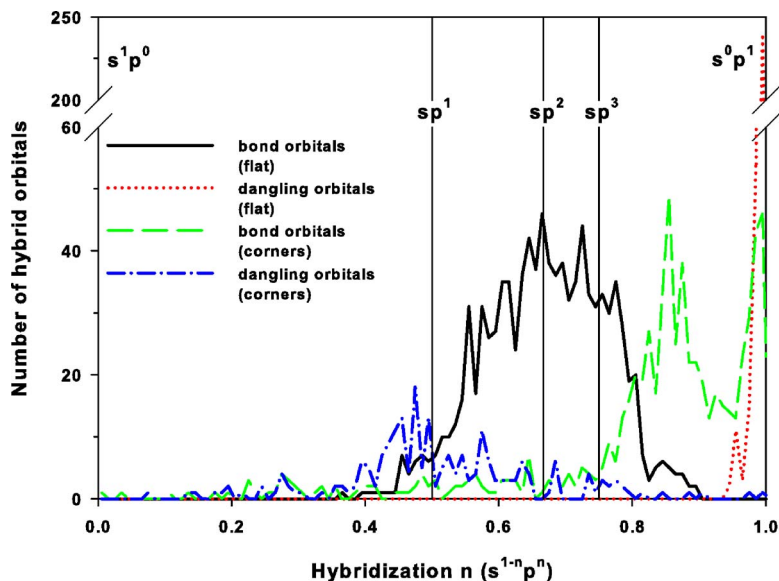
FIG. 6. (Color online) Distribution versus n of (a) the three hybridized bond orbitals for near-planar atoms (solid line), (b) the dangling orbital for the same atoms (dotted line), (c) the bond orbitals for the atoms at sharp corners (dashed line), and (d) the dangling orbitals for the same atoms (dot-dashed line), for the 17 Si_{38} isomers (OTBMD method).

The hybridized orbital $|h\rangle = \sqrt{1-n}|s\rangle + \sqrt{n}|p\rangle$ may be written in a compact form as $s^{1-n}p^n$, where $n/(1-n)$ is its hybridization. The corresponding values of n for the sp^1, sp^2, and sp^3 hybridized orbitals are 0.5, 0.666, and 0.75, respectively. In addition, $n=0$ and $n=1$ correspond to the pure $|s\rangle$ and pure $|p\rangle$ orbitals, respectively.

In Fig. 6, the distributions versus n of the three hybridized bond orbitals and dangling-bond orbitals (OTBMD) are presented. The plot confirms that the hybridizations of the atoms that have moved inward are sp^2-like, while their corresponding dangling-bond orbitals are almost pure p orbitals. In contrast, the bond and the dangling-bond orbitals of the atoms at the sharp corners have a very strong p and s characters, respectively. Their dangling bonds retain hybridization close to sp^1. Comparing the distributions shown in Fig. 5 with the corresponding distributions of the 38:9 isomer only (see Fig. 4 of Ref. 40), it can be seen that there is nothing particular in hybridization which would pick out isomer 38:9 uniquely from the others. Especially, for the atoms at sharp corners, construction of the hybrid orbitals is not always possible due to the restriction on bond angles θ_{ij}, i.e., $\cos\theta_{12}\cos\theta_{23}\cos\theta_{31} < 0$. These cases are excluded from the distributions of Fig. 6.

IV. SUMMARY AND CONCLUSIONS

In the present work, we have found the 17 optimum Si_{38} fullerene isomers, which are constructed with permutations among their pentagons and hexagons, using a global optimization method. Within this method, the 17 Si_{38} isomers were firstly optimized using an OTBMD method, and the optimum

structures found were further optimized with two more accurate but more time-consuming methods, namely, the GT-BMD and the DFT at the B3LYP/DZP level. For comparison, the same calculations were carried out for the Si_{20} fullerene. The main conclusions of our investigation are the following.

All of the Si_{38} fullerene isomers lie in almost isoenergetic local minima. The cohesive energies are concentrated in an energy range of less than 0.06 eV. On optimization, all isomers have the trivial symmetry. Of the 17 Si_{38} fullerene isomers, isomer 9, which has three distinct fused quadruples of pentagons, is energetically optimal. Distributions of pentagon and hexagon bond angles, for the 17 Si_{38} fullerene isomers, are bimodal. Half of the atoms of every Si_{38} fullerene isomer move radially inward and become almost coplanar to their nearest neighbors with sp^2-like bonding, while the others move radially outward to form sharp corners and use p-like bonding.

*Electronic address: fthenak@iesl.forth.gr

†Associated with Organic Chemistry and Catalysis.

[1] H. W. Kroto, J. R. Heath, S. C. O'Brien, R. F. Curl, and R. E. Smalley, Nature (London) **318**, 162 (1985).

[2] P. W. Fowler and D. E. Manolopoulos, *An Atlas of Fullerenes* (Clarendon, Oxford, 1995).

[3] E. Albertazzi, C. Domene, P. W. Fowler, T. Heine, G. Seifert, C. V. Alsenoy, and F. Zerbetto, Phys. Chem. Chem. Phys. **1**, 2913 (1999).

[4] B. X. Li, P. L. Cao, and D. L. Que, Phys. Rev. B **61**, 1685 (2000).

[5] M. Menon and K. R. Subbaswamy, Chem. Phys. Lett. **219**, 219 (1994).

[6] B. Marsen and K. Sattler, Phys. Rev. B **60**, 11593 (1999).

[7] A. N. Andriotis, G. Mpourmpakis, G. E. Froudakis, and M. Menon, New J. Phys. **4**, 78 (2002).

[8] A. S. Barnard and S. P. Russo, J. Phys. Chem. B **107**, 7577 (2003).

[9] R. Q. Zhang, S. T. Lee, C. K. Law, W. K. Li, and B. K. Teo, Chem. Phys. Lett. **364**, 251 (2002).

[10] M. Menon, N. N. Lathiotakis, and A. N. Andriotis, Phys. Rev. B **56**, 1412 (1997).

[11] V. Kumar and Y. Kawazoe, Phys. Rev. Lett. **87**, 045503 (2001).

[12] C. Ray, M. Pellarin, J. L. Lermé, J. L. Vialle, M. Broyer, X. Blase, P. Mélinon, P. Kéghélian, and A. Perez, Phys. Rev. Lett. **80**, 5365 (1998).

[13] A. San-Miguel, P. Kéghélian, X. Blase, P. Mélinon, A. Perez, J. P. Itié, A. Polian, E. Reny, C. Cros, and M. Pouchard, Phys. Rev. Lett. **83**, 5290 (1999).

[14] A. San-Miguel and P. Toulemonde, High Press. Res. **25**, 159 (2005).

[15] M. Menon and K. R. Subbaswamy, Phys. Rev. B **51**, 17952 (1995).

[16] J. Zhao, J. Wang, J. Jellinek, S. Yoo, and X. C. Zeng, Eur. Phys. J. D **34**, 35 (2005).

[17] Q. Sun, Q. Wang, P. Jena, B. K. Rao, and Y. Kawazoe, Phys. Rev. Lett. **90**, 135503 (2003).

[18] X. G. Gong, Phys. Rev. B **52**, 14677 (1995).

[19] U. Rothlisberger, W. Andreoni, and M. Parinello, Phys. Rev. Lett. **72**, 665 (1994).

[20] Q. Sun, Q. Wang, T. M. Briere, V. Kumar, Y. Kawazoe, and P. Jena, Phys. Rev. B **65**, 235417 (2002).

[21] T. Nagano, K. Tsumuraya, H. Eguchi, and D. J. Singh, Phys. Rev. B **64**, 155403 (2001).

[22] L. Turker, J. Mol. Struct.: THEOCHEM **548**, 185 (2001).

[23] L. Turker, J. Mol. Struct.: THEOCHEM **546**, 45 (2001).

[24] L. Turker, ACH-Models Chem. **137**, 511 (2000).

[25] V. Kumar and Y. Kawazoe, Phys. Rev. Lett. **90**, 055502 (2003).

[26] B. X. Li, P. L. Cao, B. Song, and Z. Z. Ye, J. Mol. Struct.: THEOCHEM **620**, 189 (2003).

[27] F. S. Khan and J. Q. Broughton, Phys. Rev. B **43**, 11754 (1991).

[28] B. X. Li, M. Jiang, and P. L. Cao, J. Phys.: Condens. Matter **11**, 8517 (1999).

[29] J. Leszczynski and I. Yanov, J. Phys. Chem. A **103**, 396 (1999).

[30] Z. Chen, H. Jiao, G. Seifert, A. H. C. Horn, D. Yu, T. Clark, W. Thiel, and P. von Raugé Schleyer, J. Comput. Chem. **24**, 948 (2003).

[31] X. G. Gong and Q. Q. Zheng, Phys. Rev. B **52**, 4756 (1995).

[32] B. X. Li and P. L. Cao, J. Phys.: Condens. Matter **13**, 10865 (2001).

[33] Q. Sun, Q. Wang, P. Jena, S. Waterman, and Y. Kawazoe, Phys. Rev. A **67**, 063201 (2003).

[34] J. G. Han, Z. Y. Ren, L. S. Sheng, Y. W. Zhang, J. A. Morales, and F. Hagelberg, J. Mol. Struct.: THEOCHEM **625**, 47 (2003).

[35] Z. G. Fthenakis (unpublished).

[36] Z. G. Fthenakis, R. W. A. Havenith, M. Menon, and P. W. Fowler, J. Phys.: Conf. Ser. **10**, 117 (2005).

[37] A. N. Andriotis, M. Menon, G. E. Froudakis, Z. Fthenakis, and J. E. Lowther, Chem. Phys. Lett. **292**, 487 (1998).

[38] M. Menon and K. R. Subbaswamy, Phys. Rev. B **55**, 9231 (1997).

[39] M. F. Guest, I. J. Bush, H. J. J. van Dam, P. Sherwood, J. M. H. Thomas, J. H. van Lenthe, R. W. A. Havenith, and J. Kendrick, Mol. Phys. **103**, 719 (2005).

[40] See EPAPS Document No. E-PRBMDO-75-180711 for supplementary information files. For more information on EPAPS, see http://www.aip.org/pubservs/epaps.html.

[41] The isomer numbering is the same with the one used in Fig. 1.

[42] C. P. R. Viennois, P. Toulemonde, and A. San-Miguel, J. Phys.: Condens. Matter **17**, L311 (2005).

[43] R. C. Haddon, J. Am. Chem. Soc. **108**, 2837 (1986).